Vibrio alginolyticus VepA Induces Lysosomal Membrane Permeability and Cathepsin-Independent Cell Death

Running title: *Vibrio alginolyticus* VepA and Cell Death

Agus Eka Darwinata[a], Kazuyoshi Gotoh （後藤 和義）[a]*, Takehiko Mima（美間 健彦）[a] , Yumiko Yamamoto（山本 由弥子）[a], Kenji Yokota（横田 憲治）[b] and Osamu Matsushita（松下 治）[a]

[a] *Department of Bacteriology, Okayama University Graduate School of Medicine, Dentistry and Pharmaceutical Sciences,* [b] *Graduate School of Health Sciences, Okayama University, Okayama 700-8558, Japan.*

[a] The institution where the study was conducted.

*Correspondence: Kazuyoshi Gotoh, Department of Bacteriology, Okayama University Graduate School of Medicine, Dentistry and Pharmaceutical Sciences, 2-5-1 Shikata-cho, Kita-ku, Okayama, Okayama 700-8558, Japan.

Phone: +81-86-235-7158

Fax: +81-86-235-7162

Email: gotok@okayama-u.ac.jp

Abstract

The bacterium *Vibrio alginolyticus*, an opportunistic pathogen in humans, has a type III secretion system (T3SS) that is responsible for its cytotoxicity toward eukaryotic cells. The effector of T3SS that is responsible for the cytotoxicity had not been identified. Here we demonstrate that VepA, a homolog of the T3SS effector in *V. parahaemolyticus*, is required for cytotoxicity in *V. alginolyticus*. VepA induces lysosomal membrane permeabilization, and it allows the leakage of only small molecules into the cytosol. Our findings revealed that VepA induces cathepsin-independent cell death in mammalian cells. The ferrous ion, one of the small molecules in the lysosome contents, appears to be involved in the cell death caused by *V. alginolyticus* VepA.

Keywords: cell death, lysosomal membrane permeability, VepA, *Vibrio alginolyticus*

Introduction

Vibrio alginolyticus is a halophilic, Gram-negative rod-shaped bacterium naturally distributed in marine and estuarine waters. This bacterium is known as an opportunistic pathogen for both humans and marine animals [1–3]. In humans, it causes medical problems such as wound infection [4–7], ear infection [8–12], and eye infection [13–15]. The incidence of *V. alginolyticus* infection was reported to be increasing, and this infection may develop into an emerging disease due to climate change issues [16]. A complete understanding of the virulence mechanism of *V. alginolyticus* is necessary to prevent future outbreaks.

The pathogenicity of *V. alginolyticus* has been described both *in vivo* (lethality in a mouse model) [17] and *in vitro* (cytotoxic activity toward several mammalian cell lines) [18]. The killing potency shown in those studies indicated that *V. alginolyticus* possesses virulence factor(s) that allow infection through the ability to overcome antibacterial immune responses such as phagocytosis, and the ability to obtain nutrition from the dead cells. As such a virulence factor in *V. alginolyticus*, Zhao *et al*. [17] reported that the deletion of type III secretion system (T3SS) apparatus gene reduces the cytotoxicity toward mammalian cell lines. A T3SS is a syringe-like apparatus that introduces specific proteins known as effectors into the cytoplasm of eukaryotic host cells. Injected effectors allow bacteria to manipulate the host cells' functions and cause diseases [19–21]. A variety of effectors are known to show specific cytotoxicity mechanisms in various bacterial species, but the effector of T3SS that is responsible for the cytotoxicity in *V. alginolyticus* has been unclear.

The *V. alginolyticus* T3SS gene cluster is evolutionally close to T3SS1 in *V. parahaemolyticus*, which is dominantly responsible for cytotoxicity [22]. Another T3SS in *V. parahaemolyticus*, T3SS2, which is involved in enterotoxicity, is absent in *V. alginolyticus*. Among the effectors of T3SS1 in *V. parahaemolyticus*, VepA (which has also been referred to as VopQ and as VP1680) plays a significant role in its cytotoxicity [23, 24]. Since

V. alginolyticus has a gene encoding a VepA homolog in the T3SS gene cluster, we hypothesized that the VepA homolog also has an important contribution to the cytotoxicity.

In this study, we constructed a *vepA*-deletion mutant in *V. alginolyticus* to analyze its role in the cytotoxicity of *V. alginolyticus*. We observed that *V. alginolyticus* infection led to size-specific lysosome membrane permeabilization (LMP) in a VepA-dependent manner. We also use our results in a discussion of why the small-molecule leakage from lysosomes is related to cell death in *V. alginolyticus* infection.

Materials and Methods

Bacterial strains, plasmids, and culture conditions

The bacterial strains and plasmids used in this study are listed in Table 1. We used *V. alginolyticus* ATCC 17749 [25] as the parent strain for the construction of gene-deletion mutant. We used the *Escherichia coli* DH5α [26] for general plasmid manipulation; *E. coli* DH5α(λ*pir*) was used to amplify the R6K-origin-containing plasmids, and *E. coli* RHO3 [27] was used as a conjugation donor for *V. alginolyticus*. *V. alginolyticus* strains were routinely cultured in Luria-Bertani (LB) 3% NaCl medium (1% tryptone, 0.5% yeast extract, 3% NaCl) at 37°C, and the *E. coli* strains were grown in LB medium (Lennox) (1% tryptone, 0.5% yeast extract, 0.5% NaCl) at 37°C. *E. coli* RHO3 was grown in LB medium supplemented with 100 μg/ml 2,6-diaminopimelic acid. Chloramphenicol (30 μg/ml), ampicillin (50 μg/ml), or kanamycin (100 μg/ml) was added to grow bacteria harboring the plasmid containing the corresponding resistance gene.

HeLa cells were cultured in Dulbecco's modified Eagle's medium (DMEM, Sigma, St. Louis, MO) supplemented with 10% (v/v) inactivated fetal bovine serum (FBS) (Biowest, Nuaillé, France) at 37°C under 5% CO_2. DMEM or minimum essential medium/Earle's

balanced salts (MEM/EBSS, Gibco, Grand Island, NY) without phenol red supplemented with 10% (v/v) inactivated FBS was used during incubation in the infection experiment.

Construction of a mobilizable vector for gene replacement

We constructed a mobilizable vector for gene replacement carrying the recognition site of meganuclease I-*Sce*I, pKU66, by inserting the *oriT* region into pSG76-C [28] at the *Not*I site. We amplified the *oriT* region from pUC18T-mini-Tn*7*T-Gm [29] using primers P064 (5'-GCGGCCGCTATCAGAGCTTATCGGCCAG-3'; the underlining indicates a *Not*I site) and P065 (5'-GCGGCCGCGGGGATTCCTTAAGGTATAC-3'; the underlining indicates a *Not*I site).

Construction of mobilizable vectors for gene expression

We constructed pEX18Km by replacing the ampicillin resistance gene on pEX18Ap [30] with the kanamycin resistance gene at the *Aat*II and *Ahd*I sites. We amplified the kanamycin marker from pHSG298 (Takara Bio, Shiga, Japan) using primers P394 (5'-GACGTCGATCTGATCCTTCAACTCAG-3'; the underlining indicates an *Aat*II site) and P395 (5'-GACTCCCCGTCTGCTCTGCCAGTGTTACAAC-3'; the underlining indicates an *Ahd*I site).

We constructed pHSG398T by inserting *oriT* into the *Afl*III site of pHSG398 (Takara Bio). The *oriT* region was amplified by using primers P127 (5'-ACATGTATCAGAGCTTATCGGCCAG-3'; the underlining indicates an *Afl*III site) and P128 (5'-ACATGTGGGGATTCCTTAAGGTATAC-3'; the underlining indicates an *Afl*III site).

Construction of an I-SceI expression vector

We amplified the promoter region of the elongation factor thermo unstable (EF-Tu) in *V. alginolyticus* I.029 by using primers P406 (5'- GAATTCAGCGGGTTACCCTGTACTAG-3'; the underlining indicates an *Eco*RI site) and P407 (5'-GATCGTGTTCCTTCCTAGTTATG-3').

The I-*Sce*I gene was amplified from pST76-ASceP [28] with the use of the primers P408 (5'-CATAACTAGGAAGGAACACGATCATGCATCAAAAAAACCAGGTA-3'; the underlining indicates a sequence overlapping to the 3' region of the EF-Tu promoter) and P409 (5'-CAAAGGGAAAACTGTCCATAC-3'). The two DNA fragments were spliced by overlap extension polymerase chain reaction (PCR). The recombinant fragment was ligated into pGEM-T Easy (Promega, Madison, WI) to obtain pOU246. We cloned an *Eco*RI-*Sph*I fragment of pOU246 carrying the I-*Sce*I gene with the EF-Tu promoter into the same sites of pEX18Km, resulting in pOU257.

Construction of a vepA-deletion mutant and a vscC-deletion mutant

We constructed Δ*vepA* as described [28] with several modifications. A DNA fragment with the *vepA*-deletion was constructed by overlap extension PCR as described [31] used the following primers: P787 (5'-GGATCCAACGTGGAGTAAGGATGTGAAAA-3'; underlining indicates a *Bam*HI site), P788 (5'-TGAAATTACACCCAGCCTTCTGCGCTGATTTTTTGTGTTGTATTAACCAT-3'; underlining indicates complementary region to P789), P789 (5'-GCAGAAGGCTGGGTGTAATTTCA-3') and P790 (5'-GAGCTCGAAGTCACTGAAGAGAGATTTTCGA-3'; underlining indicates a *Sac*I site).

We cloned this fragment into pKU66 at the *Bam*HI and *Sac*I sites, resulting in pOU549. *E. coli* RHO3 harboring plasmid pOU549 was conjugated with *V. alginolyticus* ATCC 17749, and the resultant transconjugant was conjugated to *E. coli* RHO3 harboring pOU257. The

transconjugants were selected on LB 2% NaCl agar plates containing antibiotic for the responsible plasmid. The *vepA*-deletion was confirmed by colony PCR using primers P787 and P790, and by sequencing of the PCR products. The remaining pOU257 was eliminated by inoculation into LB 3% NaCl medium containing 5% sucrose.

The construction of Δ*vscC* was performed using the same method as that used for the Δ*vepA* construction. The primers used to amplify the *vscC*-deletion fragment were P793 (5'-GAATTCCGGTTGCGAAAGTATGGCAATG-3'; the underlining indicates an *Eco*RI site), P794 (5'-AGGAACAACACTCACTGCGCATA-3'), P795 (5'-TATGCGCAGTGAGTGTTGTTCCTCGCCCTTCAGAGGAGTCTTAACC-3'; the underlining indicates complementary region to P794) and P796 (5'-GGATCCGCAGATCGAGTTTCTGTGTTCGG-3'; the underlining indicates a *Bam*HI site). This fragment was cloned into pKU66 at *Eco*RI and *Bam*HI sites, resulting in pOU553. The *vscC* deletion was confirmed by colony PCR using primers P793 and P796 and by sequencing of the PCR products.

Construction of a vepA expression vector

We amplified the DNA fragment containing *vepA* from the gDNA by using primers P791 (5'-GCTGAATTCAATGGTTAATACAACACAAAAAATCAGCCAAAGC-3'; underlining indicates an *Eco*RI site) and P792 (5'-GCTGGATCCTTACACCCAGCCTTCTGCCAAG-3'; underlining indicates a *Bam*HI site). The PCR product was cloned into *Eco*RI and *Bam*HI sites of pHSG398T, which yielded pOU550.

Cytotoxicity assay

HeLa cells were seeded into a 96-well plate at 3×10^4 cells/well, and then incubated at 37°C under 5% CO_2 for 48 hr. The cells were washed with DMEM or MEM/EBBS medium

without phenol red, and then infected with *V. alginolyticus* at a multiplicity of infection (MOI) of 100 for 4 hr. A ten-times dilution of *V. alginolyticus* at the optical density at 600 nm (OD_{600}) of 1.0 is equal to $3–4\times10^8$ CFU/ml on an LB 1% NaCl agar plate. We added 10 μl of these dilution cultures to $3–4\times10^4$ of HeLa cell culture to obtain the MOI of 100.

We measured the release of lactate dehydrogenase (LDH) into the medium by using a Cytotoxicity Detection Kit^{PLUS} (LDH) (Roche, Mannheim, Germany) according to the manufacturer's instructions. The percentage of LDH release was calculated based on the following equation: [OD_{490} of experimental release – OD_{490} of spontaneous release]/(OD_{490} of maximum release – OD_{490} of spontaneous release) × 100. The spontaneous release is the amount of LDH released from the cytoplasm of uninfected cells, and the maximum release is the total amount of LDH released upon the complete lysis of uninfected cells.

AO relocation assay

The acridine orange (AO) relocation assay was performed as described [24]. We used fluorescence microscopy (Biozero BZ-8000, Keyence, Tokyo) to analyze the AO-stained cells.

Fluorescent-dextran translocation

Fluorescent-dextran translocation was observed as described [32]. Before infection, HeLa cells were incubated in 100 μg/ml fluorescein isothiocyanate (FITC)-dextran for 16 hr. We analyzed fluorescent dextran in the HeLa cells by fluorescence microscopy.

Inhibition of cathepsin and reactive oxygen species (ROS), LMP induction, and iron chelation

HeLa cells were pretreated with 100 μM E-64d, a broad-spectrum cathepsin inhibitor, for 16

hr before infection. The cells were challenged with 3 mM L-Leucyl-L-Leucine methyl ester (LLOMe) for 4 hr to induce LMP. To chelate iron, we used 100 μM 2,2'-bipyridyl (BIP). To inhibit reactive oxygen species (ROS), we used 5 mM N-acetyl cysteine (NAC) or 250 μM Trolox.

Statistical analysis

The two-tailed Student's *t*-test was used for the statistical analyses.

Results

VepA contributes to HeLa cell cytotoxicity in V. alginolyticus infection

We chose *V. alginolyticus* strain ATCC17749, which was shown to be highly virulent in an *in vivo* infection model [18]. VepA (N646_0746) in this strain is homologous to that in *V. parahaemolyticus*, with 88% sequence similarity (435 aa/493 aa).

To examine the contribution of VepA to the cytotoxicity toward human cells, we performed the LDH release cytotoxicity assay after 4 hr of bacterial infection against HeLa cells (Fig. 1). The T3SS apparatus gene mutant, Δ*vscC*, showed significantly less cytotoxicity than the wild-type (WT). Δ*vepA* also showed significantly less cytotoxicity. The *vepA* complimentary strain, Δ*vepA/vepA* completely restored the cytotoxicity (similar to the WT), whereas Δ*vepA/*vector did not. To test the results of the LDH release cytotoxicity assay, we also performed propidium iodine (PI) staining. The results were similar to those of the LDH release cytotoxicity assay (data not shown). These results indicate that mainly VepA is responsible for the cytotoxicity of *V. alginolyticus*.

VepA in V. alginolyticus induced lysosomal membrane permeabilization (LMP)

213 It was reported that *V. parahaemolyticus* VepA induces LMP in mammalian cells [24, 33].
214 Here we therefore examined the integrity of lysosomes in *V. alginolyticus*-infected cells by
215 using acridine orange (AO) (Fig. 2). AO is a metachromatic dye that emits red fluorescence at
216 low pH (e.g., in lysosomes) and emits green fluorescence at neutral pH (e.g., in the cytosol)
217 [34].

218 In uninfected HeLa cells, we observed small red fluorescent dots, which reflect an
219 accumulation of the dye in lysosomes. In the WT infection, the appearance of red dots was
220 disappeared and the intensity of the green fluorescence in the cytosol was increased. In
221 contrast, in the Δ*vepA* infection, the appearance of red dots was comparable to that in the
222 uninfected cells, and the green fluorescence enhancement was not observed. In the
223 Δ*vepA/vepA* infection, the fluorescence pattern reverted to one similar to that obtained with
224 the WT. These results indicate that *V. alginolyticus* infection induces the leakage of the
225 lysosomal contents into the cytosol in a VepA-dependent manner.

226 We observed that infection with either *V. alginolyticus* strain induced a morphological
227 change of HeLa cells, i.e., cell rounding (Fig. 2). Since the Δ*vepA* infection also induced cell
228 rounding, we can safely assume that this change is not due to VepA. On the other hand, the
229 Δ*vscC* strain did not affect the cell morphology (data not shown). Therefore, this change
230 might be caused by other T3SS effectors, e.g., N646_0751, the homologue of VopS in
231 *V. parahaemolyticus* [35].

232

233 ***The VepA-induced LMP in V. alginolyticus was not due to a lysosomal membrane rupture***

234 The molecular mass of AO is approx. 0.3 kDa. To determine whether VepA induces the
235 release of only small molecules or lysosomal rupture, we observed the LMP in
236 *V. alginolyticus* infection using larger molecules: FITC-dextran, with the molecular mass of 4
237 or 10 kDa. It is well known that such macromolecules can be loaded into lysosomes to yield

238 green fluorescence punctates while the lysosomes are intact. When the lysosomes are
239 ruptured, the FITC-dextran is released into the cytosol to yield diffuse green fluorescence.
240 HeLa cells were treated with FITC-dextran for 16 hr to allow lysosomal uptake before
241 infection or challenge with an LMP inducer, LLOMe. When FITC-dextran with the molecular
242 mass of 10 kDa was preloaded (Fig. 3A), LLOMe-treated cells showed diffuse fluorescence
243 enhancement in the cytosol. In contrast, the cells infected with the WT or Δ*vepA* did not
244 exhibit the fluorescence diffusion into the cytosol, but the cells did show fluorescent
245 punctates. Our experiments using FITC-dextran with the molecular mass of 4 kDa gave the
246 same pattern (Fig. 3B). These results indicate that the VepA-mediated LMP allows the
247 translocation of molecules smaller than 4 kDa.
248
249 ***VepA-dependent cytotoxicity is not due to lysosomal cathepsin***
250 LMP-associated cell death is usually related to lysosomal cathepsin release [36]. Since the
251 VepA-induced LMP in *V. alginolyticus* infection allowed the release of only molecules <4
252 kDa, we hypothesized that lysosomal proteases with the molecular sizes >4 kDa (including
253 cathepsins, the molecular masses of which is approx. 30 kDa) could not pass through the
254 lysosomal membrane. To determine whether the VepA-mediated cell death is due to cathepsin
255 release from lysosomes, we examined the effect of a broad-spectrum cathepsin inhibitor, E-
256 64d, on cell death. HeLa cells were treated with E-64d for 16 hr before challenge with
257 LLOMe or a *V. alginolyticus* strain. The lysosomal rupture induced by LLOMe subsequently
258 resulted in cell death, as reported [36], and cytotoxicity was reduced by E-64d treatment as
259 expected (Fig. 4A). When the cells were challenged with the WT strain, the cell death rates
260 were similar regardless of the E-64d treatment (Fig. 4A). These results suggest that cathepsin
261 is not the major causative factor of *V. alginolyticus* cytotoxicity.

Since the lysosome is one of the iron-rich intracellular organelles, VepA might allow excessive iron release into the cytosol to induce cell death via ROS [37]. To investigate the roles of iron and ROS in cell death in *V. alginolyticus* infection, we compared their cytotoxic effects in the presence of an iron chelator, BIP, and an ROS scavenger, NAC or Trolox. In the presence of BIP, the cytotoxicity was significantly reduced. However, after the ROS scavenger treatment, the cytotoxicity was slightly reduced or not changed, respectively (Fig. 4B). When we directly examined hydroxyl radicals by using hydroxyphenyl fluorescein, we observed no fluorescence in *V. alginolyticus*-infected cells (data not shown).

Discussion

The opportunistic pathogen *V. alginolyticus* has an active T3SS that is involved in its cytotoxicity [3, 17]. In *V. parahaemolyticus,* a T3SS effector, VepA, makes the major contribution to the cytotoxicity. Our present findings demonstrate that the VepA in *V. alginolyticus* plays a significant role in its cytotoxicity (Fig. 1). Since the *vepA* gene is conserved in several *Vibrio* species [38], it is possible that VepA-induced cell death is a common pathogenic mechanism among the species.

Our present results obtained using an *in vitro* infection model also showed that *V. alginolyticus* induces the leakage of the 0.3-kDa lysosomotropic dye AO into the cytosol in a VepA-dependent manner (Fig. 2). Molecules larger than 4 kDa were retained in the lysosomes (Fig. 3). We thus speculate that *V. alginolyticus* VepA induces size-specific LMP. These results are consistent with those obtained by Sreelatha et al. [33], i.e., *V. parahaemolyticus* VepA induces LMP, which only allows the release of molecules <4 kDa. Sreelatha et al. also proposed that VepA forms pores with an estimated diameter of 18 Å in liposomes. Further studies are necessary to determine whether *V. alginolyticus* VepA forms such pores in the lysosomal membrane.

LMP results in cell death, which is usually related to lysosomal cathepsin release [36]. Since *V. alginolyticus* VepA induced size-specific LMP, i.e., <4 kDa, we can safely assume that this is not the case, since lysosomal proteases (e.g., cathepsins) have much larger molecular masses at approx. 30 kDa. To test this, we used the broad-spectrum cathepsin inhibitor E-64d to determine whether it inhibits the cell death. Since *V. alginolyticus* VepA induced cell death regardless of the presence of this inhibitor (Fig. 4A), the cell death is caused by a factor(s) other than cathepsins. We thus suspect that the involvement of lysosomal small molecules potentially harmful to the cells is responsible for the VepA-induced cell death.

The lysosome is a pool of redox-active iron capable of generating free radicals via the Fenton reaction [37]. We used the iron chelator BIP to examine whether iron mediates the VepA-induced cell death. Since iron chelation significantly reduced the cell death to a level that was almost the same as that observed with *vepA*-deleted *V. alginolyticus* infection, it appears that iron is an important mediator of VepA-dependent cell death (Fig. 4B). Our results support the observation by Matsuda et al. [24] that an iron chelator partially reduced the cytotoxicity in *V. parahaemolyticus* infection.

Since it is well known that iron triggers cell death via ROS accumulation [37, 39], we examined the effects of ROS scavengers. NAC inhibited the cell death only slightly, but Trolox did not inhibit the cell death at all. Moreover, the growth rate of *V. alginolyticus* was not affected by the presence of BIP, NAC or Trolox. We therefore propose that iron induces cell death without ROS accumulation in this infection model. A study on yeast demonstrated that iron overload stimulates the sphingolipid production that leads to cell death, without ROS accumulation [37]. Additional studies are required to elucidate the function of iron in VepA-induced cell death.

In conclusion, our experiments demonstrated that VepA induced cathepsin-independent

cell death. We also observed that VepA induced size-specific LMP that allows only small molecules to be released into the cytosol. We propose that iron leakage from lysosomes plays an important role in this cell death mechanism. Further research is required to elucidate the underlying molecular mechanism, which might provide insights into the development of novel therapeutics that target the VepA-related cell death mechanism.

Acknowledgements

RHO3, DH5α(λ*pir*), pEX18Ap, and pUC18T-mini-Tn*7*T-Gm were kindly provided by Dr. Herbert P. Schweizer (Department of Molecular Genetics and Microbiology, Emerging Pathogens Institute, University of Florida, Gainesville, FL, USA). pSG76-C and pST76-ASceP were kindly provided by Dr. György Pósfai (Systems and Synthetic Biology Unit, Biological Research Centre of the Hungarian Academy of Sciences, Szeged, Hungary). This study was supported by a MEXT KAKENHI grant, no. JP15K19093.

References

1. Tantillo GM, Fontanarosa M, Di Pinto A and Musti M: Updated perspectives on emerging vibrios associated with human infections. Lett Appl Microbiol (2004) 39: 117–126.
2. Austin B: Vibrios as causal agents of zoonoses. Vet Microbiol (2010) 140: 310–317.
3. Zhao Z, Chen C, Hu CQ, Ren CH, Zhao JJ, Zhang LP, Jiang X, Luo P and Wang QB: The type III secretion system of *Vibrio alginolyticus* induces rapid apoptosis, cell rounding and osmotic lysis of fish cells. Microbiology (2010) 156: 2864–2872.
4. Rubin SJ and Tilton RC: Isolation of *Vibrio alginolyticus* from wound infections. J Clin Microbiol (1975) 2: 556–558.
5. Pezzlo M and Burns MJ: Wound infection associated with *Vibrio alginolyticus*. Am J

337 Clin Pathol (1979) 71:476-478.

338 6. Spark RP, Fried ML, Perry C and Watkins C: *Vibrio alginolyticus* wound infection:
339 case report and review. Ann Clin Lab Sci (1979) 9: 133–138.

340 7. Matsiota-Bernard P and Nauciel C: *Vibrio alginolyticus* wound infection after exposure
341 to sea water in an air crash. Eur J Clin Microbiol Infect Dis (1993) 12: 474–475.

342 8. Ciufecu C, Nacescu N and Florescu D: Middle ear infection due to *Vibrio*
343 *alginolyticus*. Bacteriological characterization. Acta Microbiol Acad Sci Hung (1979)
344 26: 95–98.

345 9. Dronda F, Canton R, Selma JL, Garcia-Ramos F and Martinez-Ferrer M: *Vibrio*
346 *alginolyticus* and swimmer's otitis externa. 2 cases and review of the literature. Enferm
347 Infec Microbiol Clin (1991) 9: 630–633.

348 10. Tsakris A, Psifidis A and Douboyas J: Complicated suppurative otitis media in a Greek
349 diver due to a marine halophilic *Vibrio* sp. J Laryngol Otol (1995) 109: 1082–1084.

350 11. Mukherji A, Schroeder S, Deyling C and Procop GW: An unusual source of *Vibrio*
351 *alginolyticus*-associated otitis: prolonged colonization or freshwater exposure? Arch
352 Otolaryngol Head Neck Surg (2000) 126: 790–791.

353 12. Feingold MH and Kumar ML: Otitis media associated with *Vibrio alginolyticus* in a
354 child with pressure-equalizing tubes. Pediatr Infect Dis J (2004) 23: 475–476.

355 13. Schmidt U, Chmel H and Cobbs C: *Vibrio alginolyticus* Infections in Humans. J Clin
356 Microbiol (1979) 10: 666–668.

357 14. Penland RL, Boniuk M and Wilhelmus KR: *Vibrio* ocular infections on the U.S. Gulf
358 Coast. Cornea (2000) 19: 26–29.

359 15. Li XC, Xiang ZY, Xu XM, Yan WH and Ma JM: Endophthalmitis caused by *Vibrio*
360 *alginolyticus*. J Clin Microbiol (2009) 47: 3379–3381.

361 16. Sganga G, Cozza V, Spanu T, Spada PL and Fadda G: Global climate change and

wound care: case study of an off-season *Vibrio alginolyticus* infection in a healthy man. Ostomy Wound Manage (2009) 55: 60–62.

17. Zhao Z, Zhang L, Ren C, Zhao J, Chen C, Jiang X, Luo P and Hu C: Autophagy is induced by the type III secretion system of *Vibrio alginolyticus* in several mammalian cell lines (2010) 193: 53–61.

18. Liu X-F, Zhang H, Liu X, Gong Y, Chen Y, Cao Y and Hu C: Pathogenic analysis of *Vibrio alginolyticus* infection in a mouse model. Folia Microbiol (Praha) (2014) 59: 167–171.

19. Muller S, Feldman MF and Cornelis GR: The Type III secretion system of Gram-negative bacteria: a potential therapeutic target? Expert Opin Ther Targets (2001) 5: 327–339.

20. Galán JE and Wolf-Watz H: Protein delivery into eukaryotic cells by type III secretion machines. Nature (2006) 444: 567–573.

21. Coburn B, Sekirov I and Finlay BB: Type III Secretion systems and disease. Clin Microbiol Rev (2007) 20: 535–549.

22. Hiyoshi H, Kodama T, Iida T and Honda T: Contribution of *Vibrio parahaemolyticus* virulence factors to cytotoxicity, enterotoxicity, and lethality in mice. Infect Immun (2010) 78: 1772–1780.

23. Ono T, Park K-S, Ueta M, Iida T and Honda T: Identification of proteins secreted via *Vibrio parahaemolyticus* type III secretion system 1. Infect Immun (2006) 74: 1032–1042.

24. Matsuda S, Okada N, Kodama T, Honda T and Iida T: A Cytotoxic type III secretion effector of *Vibrio parahaemolyticus* targets vacuolar H^+-ATPase subunit c and ruptures host cell lysosomes. PLoS Pathog (2012) 8: e1002803.

25. Miyamoto Y, Nakamuma K and Takizawa K: Pathogenic halophiles. Proposals of a

new genus "*Oceanomonas*" and of the amended species names. Microbiol Immunol (1961) 5: 477–486.

26. Liss L: New M13 host: DH5αF' competent cells. Focus (1987) 9: 13.

27. López CM, Rholl DA, Trunck LA and Schweizer HP: Versatile dual-technology system for markerless allele replacement in *Burkholderia pseudomallei*. Appl Environ Microbiol (2009) 75: 6496–6503.

28. Posfai G, Kolisnychenko V, Bereczki Z and Blattner FR: Markerless gene replacement in *Escherichia coli* stimulated by a double-strand break in the chromosome. Nucleic Acids Res (1999) 27: 4409–4415.

29. Choi KH, Gaynor JB, White KG, Lopez C, Bosio CM, and Karkhoff-Schweizer RR and Schweizer HP: A Tn7-based broad-range bacterial cloning and expression system. Nat Meth (2005) 2: 443–448.

30. Hoang TT, Karkhoff-Schweizer RR, Kutchma AJ and Schweizer HP: A broad-host-range Flp-FRT recombination system for site-specific excision of chromosomally-located DNA sequences: application for isolation of unmarked *Pseudomonas aeruginosa* mutants. Gene (1998) 212: 77–86.

31. Heckman KL and Pease LR: Gene splicing and mutagenesis by PCR-driven overlap extension. Nat Protoc (2007) 2: 924–932.

32. Ellegaard A-M, Jäättelä M and Nylandsted J: Visualizing lysosomal membrane permeabilization by fluorescent dextran release. Cold Spring Harb Protoc (2015) 2015: 900–903.

33. Sreelatha A, Bennett TL, Zheng H, Jiang QX, Orth K and Starai VJ: *Vibrio* effector protein, VopQ, forms a lysosomal gated channel that disrupts host ion homeostasis and autophagic flux. Proc Natl Acad Sci USA (2013) 110: 11559–11564.

34. Pierzynska-Mach A, Janowski PA and Dobrucki JW: Evaluation of acridine orange,

412 LysoTracker Red, and quinacrine as fluorescent probes for long-term tracking of acidic
413 vesicles. Cytometry A (2014) 85: 729–737.
414 35. Yarbrough ML, Li Y, Kinch LN, Grishin NV, Ball HL and Orth K: AMPylation of
415 Rho GTPases by *Vibrio* VopS disrupts effector binding and downstream signaling.
416 Science (2009) 323: 269–272.
417 36. Droga-Mazovec G, Bojic L, Petelin A, Ivanova S, Romih R, Repnik U, Salvesen GS,
418 Stoka V, Turk V and Turk B: Cysteine cathepsins trigger caspase-dependent cell death
419 through cleavage of bid and antiapoptotic Bcl-2 homologues. J Biol Chem (2008) 283:
420 19140–19150.
421 37. Dixon SJ and Stockwell BR: The role of iron and reactive oxygen species in cell death.
422 Nat Chem Biol (2013) 10: 9–17.
423 38. Park KS, Ono T, Rokuda M, Jang MH, Okada K, Iida T and Honda T: Functional
424 characterization of two type III secretion systems of *Vibrio parahaemolyticus*. Infec
425 Immun (2004) 72: 6659–6665.
426 39. Kurz T, Eaton JW and Brunk UT: The role of lysosomes in iron metabolism and
427 recycling. Int J Biochem Cell Biol (2011) 43: 1686–1697.
428

429 **Table 1.** Bacterial strains and plasmids

Strain/Plasmid	Relevant Genotype or Properties	Reference or Source
***E. coli* strains**		
DH5α	F⁻ Φ80*lacZ*ΔM15 Δ(*lacZYA-argF*)*U169 deoR recA1 endA1 hsdR17*(r_K^- m_K^-) *phoA supE44*	[26]
DH5α(*λpir*)	DH5α *λpir*	H.P. Schweizer
RHO3	SM10(*λpir*) Δ*asd*:*FRT* Δ*aphA*:*FRT*	[27]
***V. alginolyticus* strains**		
ATCC 17749	Wild-type strain	[25]
Δ*vepA*	ATCC 17749 Δ*vepA*	This study
Δ*vscC*	ATCC 17749 Δ*vscC*	This study
Δ*vepA/vepA*	Δ*vepA* harboring pOU550	This study
Δ*vepA/*vector	Δ*vepA* harboring pHSG398T	This study
Plasmids		
pGEM-T Easy	AMP^r; TA cloning vector	Promega
pSG76-C	CM^r; Suicide plasmid vector; I-*Sce*I	[28]
pKU66	CM^r; pSG76-C with *oriT*	This study
pHSG398	CM^r; pUC-type cloning vector	Takara Bio.
pHSG398T	CM^r; pHSG398 with *oriT*	This study
pEX18Ap	AMP^r; cloning vector; *sacB*; *oriT*	[30]
pEX18Km	KM^r; pEX18Ap with AMP^r replacement to KM^r	This study
pHSG298	KM^r; source of kanamycin resistance gene	Takara Bio.
pUC18T-mini-Tn*7*T-Gm	AMP^r, GM^r; source of *oriT*	[29]

pST76A-SceP	AMP^r; source of I-*Sce*I	[28]
pOU246	AMP^r; pGEM-T Easy with EF-Tu promoter and I-*Sce*I	This study
pOU257	KM^r; pEX18Km with EF-Tu promoter and I-*Sce*I	This study
pOU549	CM^r; pKU66 with Δ*vepA* recombinant DNA fragment	This study
pOU550	CM^r; pHSG398T with *vepA*	This study
pOU553	CM^r; pKU66 with Δ*vscC* recombinant DNA fragment	This study

AMP, ampicillin; CM, chloramphenicol; GM, gentamycin; KM, kanamycin.

FIGURE LEGENDS

Fig. 1. VepA contribution to cytotoxicity toward HeLa cells. HeLa cells were infected with the wild-type strain (WT), a *vscC*-deletion mutant (Δ*vscC*), a *vepA*-deletion mutant (Δ*vepA*), or a *vepA*-deletion mutant carrying a *vepA*-expression plasmid or the empty vector (Δ*vepA*/*vepA* or Δ*vepA*/vector, respectively). We evaluated cytotoxicity at 4 hr after infection by measuring the amount of LDH released into the culture supernatant. Data are mean±SD. ***P<0.001.

Fig. 2. AO relocation assays results. HeLa cells were incubated with AO and then infected with the WT strain, a *vepA*-deletion mutant (Δ*vepA*), or a *vepA*-deletion mutant carrying a *vepA*-expression plasmid (Δ*vepA*/*vepA*) for 4 hr. AO emits red fluorescence in the lysosomes and green fluorescence in the cytosol.

Fig. 3. LMP visualized by fluorescent dextran release. HeLa cells were incubated with 10-kDa (**A**) or 4-kDa (**B**) FITC-dextran for 16 hr and then challenged with LLOMe or infected with the WT strain, *vepA*-deletion mutant (Δ*vepA*), or *vepA*-deletion mutant carrying a *vepA*-expression plasmid (Δ*vepA*/*vepA*) for 4 hr.

Fig. 4. Cytotoxicity of *V. alginolyticus* infection in cathepsin inhibition, iron chelation, and ROS inhibition. **A**, HeLa cells were pretreated with E-64d (E) and then challenged with 3 mM LLOMe or infected with the WT strain for 4 hr. **B**, HeLa cells were pretreated with an iron chelator (BIP) or an ROS scavenger (NAC or Trolox) and then infected with WT strain for 4 hr. Data are mean±SD. **P<0.01, ***P<0.001.

Fig. 1.

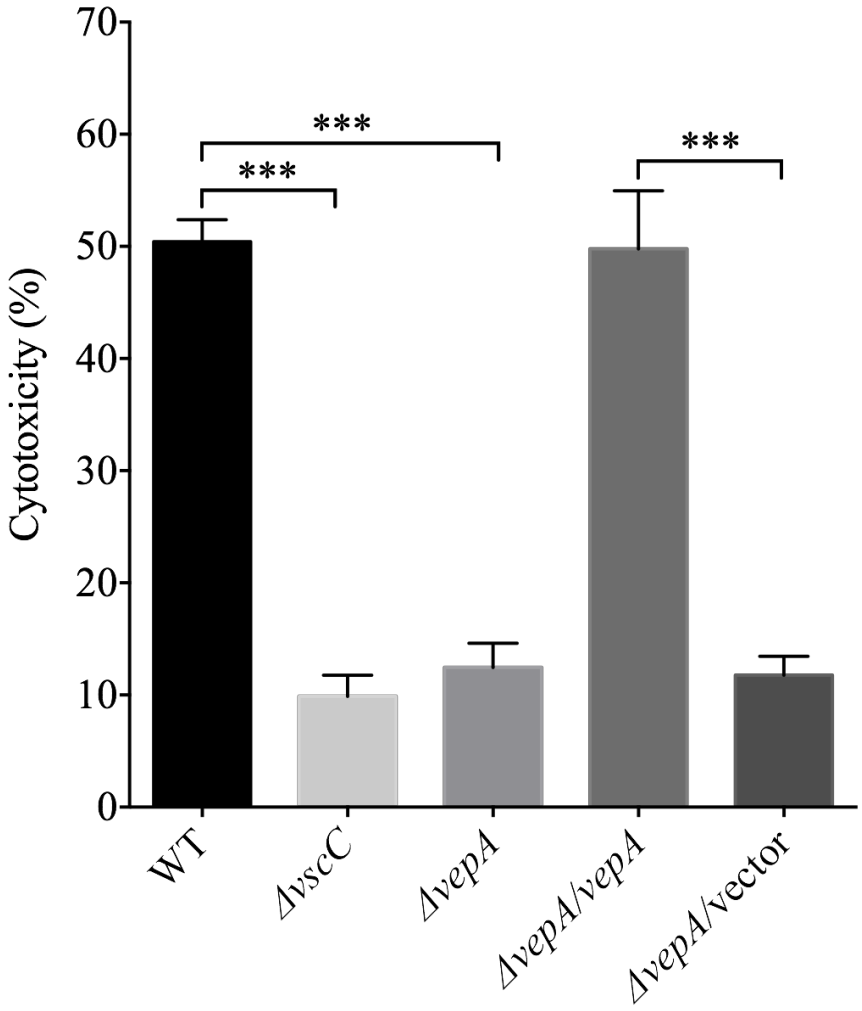
70
60
50
40
30
20
10
0
Cytotoxicity (%)
***
***
***
WT
ΔvscC
ΔvepA
ΔvepA/vepA
ΔvepA/vector

Fig. 2.

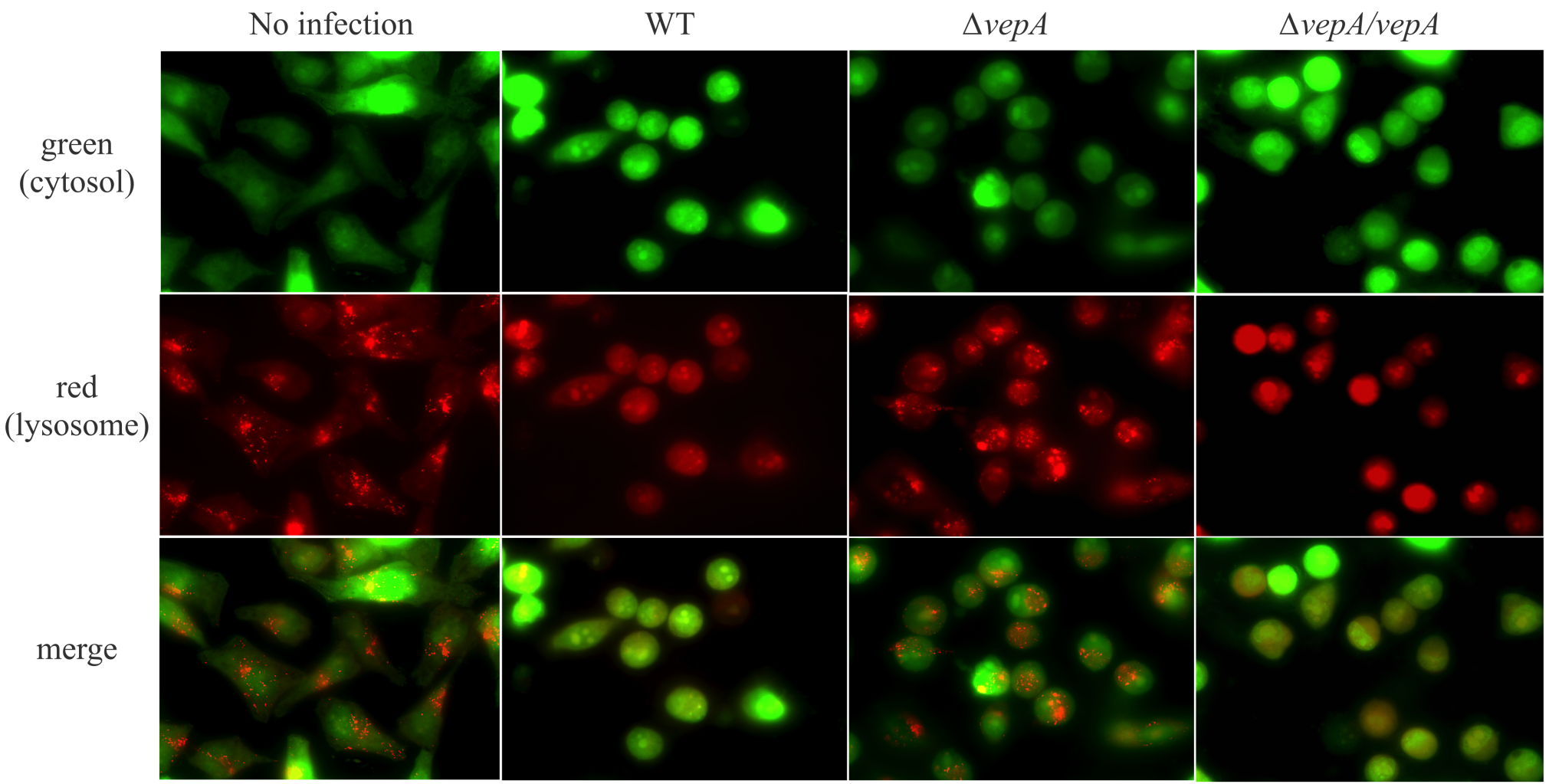
No infection
WT
ΔvepA
ΔvepA/vepA
green (cytosol)
red (lysosome)
merge

Fig. 3

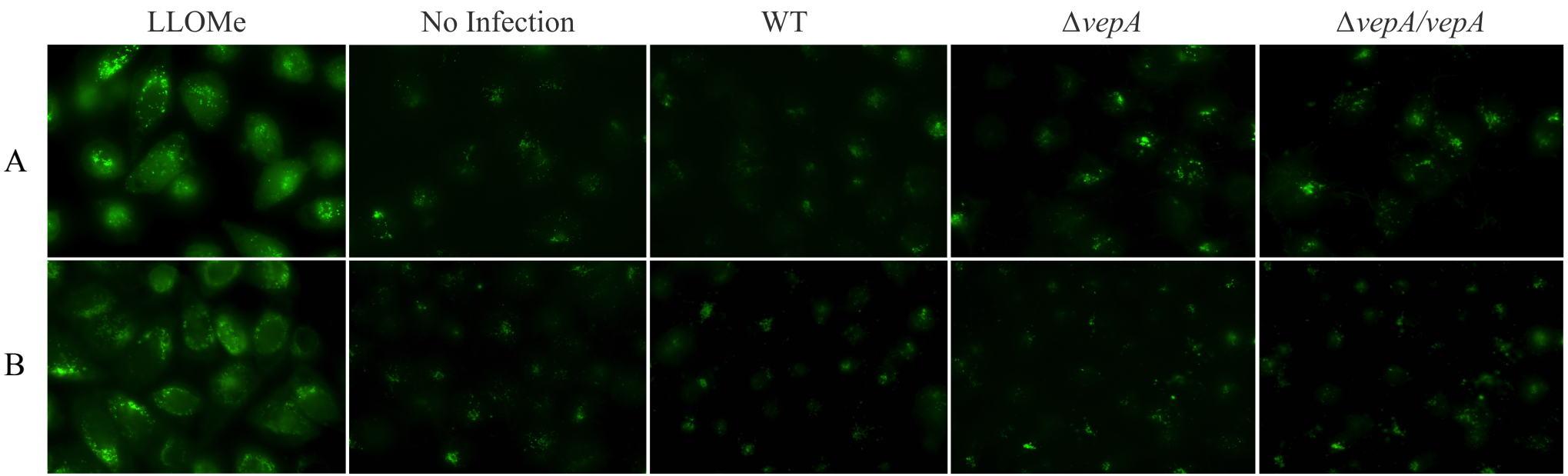

Fig. 4.

A

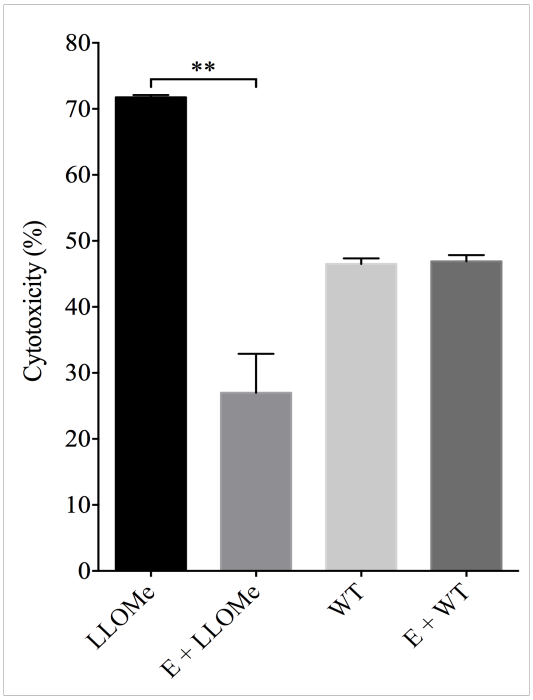
80
70
60
50
40
30
20
10
0
Cytotoxicity (%)
**
LLOMe
E + LLOMe
WT
E + WT

B

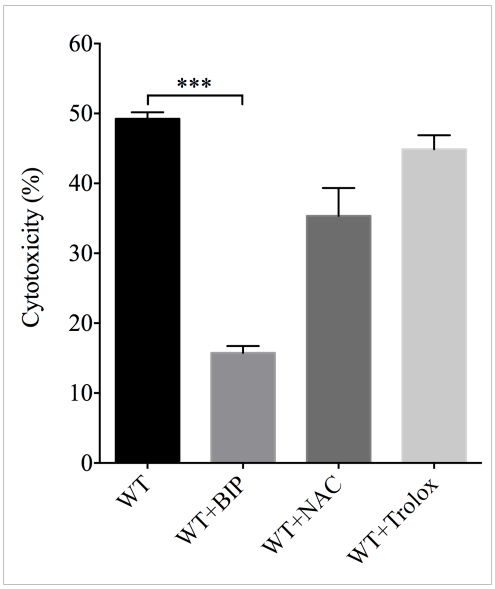
60
50
40
30
20
10
0
Cytotoxicity (%)
***
WT
WT+BIP
WT+NAC
WT+Trolox